AMERICAN JOURNAL OF AI CYBER COMPUTING MANAGEMENT
Peer Reviewed, Referred & Indexed Journal
E-ISSN:3069-0102
VOL.6, NO. 1(2026)

DETECTION OF ACUTE LYMPHOBLASTIC LEUKEMIA USING NOVEL BONE MARROW IMAGE SEGMENTATION

[1]P. APARNA, [2]Dr. V.T. VENKATESWARLU, [3]G. MOUNIKA, [4]D. PRIYANKA LAKSHMI, [5]P. SUSMITHA, [6] L. VIJITHA

[2] Professor, ECE Dept , RISE Krishna Sai Prakasam Group of Institutions, Valluru, AP
[1,3,4,5,6]Students, ECE Dept, RISE Krishna Sai Prakasam Group of Institutions, Valluru, AP
[1]ponduriaparna@gmail.com , [2]venki.vt@gmail.com, [3]gurramkondumouni@gmail.com, [4]desu3467@gmail.com,
[5]susmithapabbisetty7@gmail.com, [6]vijithalam21@gmail.com

ABSTRACT

In order to differentiate between normal and acute lymphoblastic leukemia (ALL), we describe a novel approach in this article for automating the segmentation and classification of bone marrow pictures. Building on previous segmentation methods, our method improves the dual threshold segmentation procedure, maximizing the separation of components from the cytoplasm and nucleus. By adjusting threshold values according on image properties, this is accomplished and produces better segmentation results than earlier techniques. We use mathematical morphology and median filtering approaches to overcome issues like noise and incomplete white blood cells. These techniques successfully reduce noise in the images and eliminate missing cells, resulting in more accurate and clean segmentation. Furthermore, utilizing a hybrid discrete wavelet transform, we suggest a novel feature extraction technique that captures both frequency and spatial information. This improves classification reliability by enabling the extraction of highly discriminative features from segmented images. We use an enhanced Adaptive Neuro-Fuzzy Inference System (ANFIS) that makes use of the retrieved features for categorization. Our improved classification system outperforms conventional techniques and guarantees precise acute lymphoblastic leukemia identification. Our unique approach is the thorough fusion of segmentation strategies, sophisticated denoising algorithms, new feature extraction, and enhanced classification. Our approach exhibits exceptional classification accuracy based on MATLAB 10.0 examination of bone marrow samples from the Acute Lymphoblastic Leukemia Image Database (ALL-IDB) for Image Processing database. The promise of our method as a superior tool for ALL diagnosis is further demonstrated by the segmentation accuracy for several cell types, such as Band cells (96%), Metamyelocyte (99%), Myeloblast (96%), N. myelocyte (97%), N. promyelocyte (97%), and Neutrophil cells (98%).

Keywords: blood cells, segmentation, leukemia classification, adaptive neuro-fuzzy inference system (ANFIS)

I INTRODUCTION

Microscopic pictures of blood cells are used to identify a number of illnesses. A person's blood changes

condition signify the beginning of diseases. If left untreated or ignored, leukemia can be fatal. Leukemia is the fifth most common cause of mortality for males and the sixth most common cause for women. Leukemia starts in the bone marrow. It shows the inside of each bone, including bone marrow, a thin material [1]. Platelets, white blood cells (leucocytes), and red blood cells (erythrocytes) make up the blood marrow, as illustrated in Fig. 1. White blood cells can assist detect or combat any illness or infection, including leukemia. Erythrocytes carry oxygen from the lungs to the organs and other tissues. body parts.

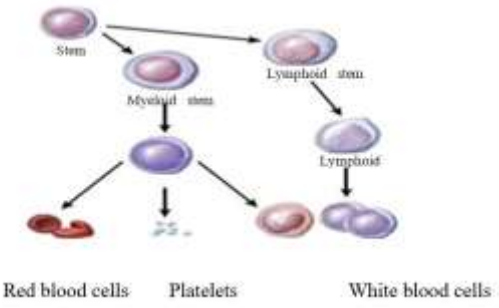


Fig.1. Stem Cell Evolution

Platelets are the components that aid in the clotting process, which in turn stops excessive bleeding. The result of bone marrow cells altering and becoming infected is leukemia, or infected cells. These leukemia cells differ from healthy ones in a

number of ways. They live longer than normal cells and have an abnormal pattern of development. Leukemia cells do not die after a certain period of time, whereas normal cells do [2]. Old leukemia cells persist for a very long time, but new leukemia cells are created incorrectly. The type of leukemia determines the rate at which the cells progress. How a stem cell can differentiate into a myeloid or lymphoid stem cell is shown in Figure 2. A myeloid blast is produced by a myeloid stem cell. Erythrocytes (red blood cells), leucocytes (white blood cells), and platelets are all produced by the myeloid blast. The cells of the lymphoid system also develop into lymphoid blasts, which generate white blood cells. The blood contains White Blood Cells (WBC) in five different types: lymphocytes, myelocytes, neutrophils, basophils, and eosinophils. Patients with leukemia have longer lifespans because the bone marrow produces aberrant white blood cells (WBCs), which grow erratically and interfere with normal cell functioning. The most effective way to save a patient's life is to detect leukemia early on. However, the traditional method of hand counting is laborious and time-consuming. Then, the Automated Hematology Counter is invented, but it is quite expensive and out of reach for developing and impoverished countries [1]. Although it depends on the application and the characteristics of the images being segmented, enhanced thresholding offers benefits over conventional segmentation methods like watershed or region growth. Conventional segmentation methods are more resilient and flexible since they can handle images with intricate structures and a wide range of intensity variations. For example, watershed segmentation can be used to segment objects that overlap or touch, whereas region expansion can be used to split things with uneven geometries. On the other hand, enhanced thresholding is a simpler and faster method that works well for images with well-defined intensity thresholds, like grayscale or binary images with definite object borders. It can also be used when the object of interest has a uniform distribution of intensity, which makes it easy to identify the object based on its intensity values. However, if the object of interest has a wide range of intensities or the intensity values are poorly defined, enhanced thresholding may result in over- or under-segmentation, therefore it may not be suitable for more complex images. This could lead to segmentation issues and impair the accuracy of ensuing analysis.

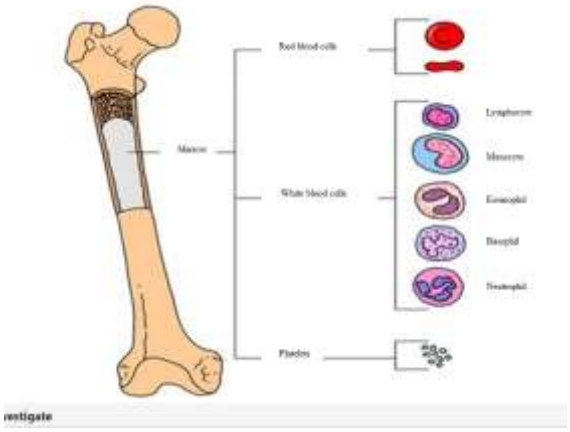


Fig.2. Bone Marrow

On order to identify defective WBCs in leukemia slides, we have developed an automated approach. For the identification and classification of leukemia cells, we employed (1) enhanced dual threshold segmentation for leukocyte cell image segmentation; (2) hybrid DWT feature extraction used for leukocyte cell image; and (3) an improved Adaptive Neuro-Fuzzy Inference System (ANFIS) classifier. As a result, computing time is cut down, and efficiency and accuracy are improved [3]. Our contributions can be summarized as follows: (1) Automated approach: The authors have developed an automated method for identifying defective WBCs in leukemia slides. This is an important contribution as it improves the efficiency and accuracy of diagnosing leukemia, which is traditionally a time-consuming and subjective process [4].

(2) Enhanced dual threshold segmentation: The authors have introduced an improved technique for segmenting leukocyte cell images called enhanced dual threshold segmentation. This method goes

beyond traditional thresholding techniques by considering both the nucleus and cytoplasm components of the blood smear images. This more accurate segmentation enables better analysis and classification of WBCs.

(3) Hybrid Discrete Wavelet Transform (DWT) feature extraction: The authors have employed a hybrid discrete wavelet transform to extract features from leukocyte cell images. This approach combines wavelet analysis and feature extraction, allowing for more comprehensive and informative characterization of the cells. The use of hybrid DWT enhances the ability to capture relevant features for classification purposes.

4. Enhanced Adaptive Neuro-Fuzzy Inference System (I-ANFIS) classifier: In their automated method, the authors have employed an improved adaptive neuro-fuzzy inference system as a classifier. This classifier efficiently distinguishes between normal and abnormal samples by fusing neural network techniques with fuzzy logic concepts. The ANFIS system's accuracy and resilience in differentiating between various WBC kinds are improved by the modifications made to it. The combination of better ANFIS classification, hybrid DWT feature extraction, and increased dual threshold segmentation for automated leukemia cell analysis is what makes this work new overall. These novel components provide potential breakthroughs in medical picture processing and illness identification while also aiding in a more precise and effective leukemia diagnosis.

II RELATED WORK

Madhloom et al. [5] employed image arithmetic operations and thresholding techniques to detect white blood cell (WBC) nuclei. A major challenge in their system was determining an appropriate segmentation threshold, as fixed thresholds were insufficient for accurately isolating WBC nuclei across varying samples. Their method integrated automatic contrast stretching, image arithmetic, minimum filtering, and global thresholding to extract the nucleus from the entire cell body. The reported accuracy ranged between 85% and 98% when validated against expert annotations. However, the segmentation performance was sensitive to image quality, staining inconsistencies, overlapping cells, and imaging artifacts. Furthermore, the method may struggle when handling abnormal or rare cell types requiring specialized analysis.

Kovalev et al. [6] proposed a technique for classifying five categories of leukocytes by first detecting nuclei and subsequently applying region-growing algorithms to extract complete cell membranes. Their method achieved recognition accuracy exceeding 98% on a dataset of 662 images collected from 22 blood samples using different imaging systems. Despite its high accuracy, the approach may be influenced by variations in imaging equipment and sample preparation procedures. Additionally, its applicability is limited to five WBC categories, potentially reducing effectiveness when dealing with rare or atypical cell types.

Scotti et al. [7] utilized low-pass filtering for background noise removal, followed by thresholding and clustering to segment WBCs under varying illumination conditions. Their strategy enhanced microscope images and enabled reliable feature extraction for leukemia diagnosis. However, the method’s performance may depend on specific microscope configurations and preparation protocols.

Piuri and Scotti [8] adopted an edge-detection-based segmentation method and trained a neural network using morphological features to differentiate lymphoblasts. Although effective, reliance solely on morphological features may limit classification accuracy, as complementary cytoplasmic or molecular characteristics are not considered.

Halim et al. [9] introduced an automated blast cell counting system but did not incorporate optimal threshold determination, feature extraction, or classification mechanisms. The absence of feature extraction and classifiers restricts its analytical depth and diagnostic reliability.

Mohapatra et al. [10] applied clustering-based segmentation and extracted multiple features, including shape, color, texture, fractal, Fourier descriptors, and contour characteristics. However, the use of a private dataset limits comparative evaluation and benchmarking against other methods.

Labati et al. [11] contributed a publicly available dataset comprising normal and leukemia blood samples, facilitating standardized testing and comparative analysis. Liao and Deng [12] proposed a threshold-based WBC extraction method assuming circular cell shapes, which may reduce segmentation accuracy for irregular morphologies.

Angulo and Flandrin [13] introduced a two-stage segmentation method combining binary filtering and automated thresholding to extract nucleus, cytoplasm, and nucleolus regions. However, variations in staining and image quality may degrade segmentation performance. Sinha and Ramakrishnam [14] proposed Gaussian Mixture Modeling with the EM algorithm for unsupervised leukocyte segmentation, though staining variations may require adaptive parameter adjustments.

Treera-Umpon [15] applied fuzzy clustering for nucleus segmentation but did not address cytoplasm extraction. Dorini et al. [16] utilized image forest transform and watershed methods, though performance was limited for non-spherical cytoplasmic structures. Comaniciu and Meer [17] used LUV color space segmentation but neglected cytoplasm extraction.

Yang et al. [18] proposed a GVF-based segmentation approach but faced challenges with weak edges and texture differentiation. Fang et al. [19] applied Particle Swarm Optimization to train a neural network for WBC classification; however, cytoplasmic nucleus recognition remained limited. Wang and Wang [21] combined thresholding, morphology, and fuzzy cellular neural networks but could not effectively separate nucleus and cytoplasm. Chinwaraphat et al. [22] introduced modified fuzzy c-means clustering, yet required manual cropping. Meurie et al. [23] proposed pixel categorization-based segmentation, though computational time increased due to multiple classifiers.

III PROPOSED WORK

The suggested work is divided into many steps, including pre-processing, segmentation, feature extraction, and classification. A median filter is used to pre-process the blood image. Enhanced dual-threshold is used to split the pre-processed image into two parts. Using the hybrid discrete wavelet transform, features are retrieved. Additionally, classification is carried out using an improved AFIS that can distinguish between normal and leukemic cells as shown in Fig. 3

Segmentation

The improved dual-threshold segmentation technique consists of three phases: pre-processing, threshold segmentation, and post-processing, as shown in Fig. 4, where I1 is the blood group, G2, G2', T1, and T2 are phases of Motosis, H, H2, and H2' are the haptoglobin phenotypes. Two images are acquired for further handling during the pre-processing stage: one is a contrast-stretched grey image, and the other is an H-part image from the modified YCbCr colour space[24]

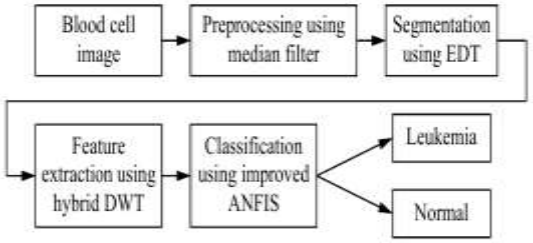


Fig. 3 Proposed work.

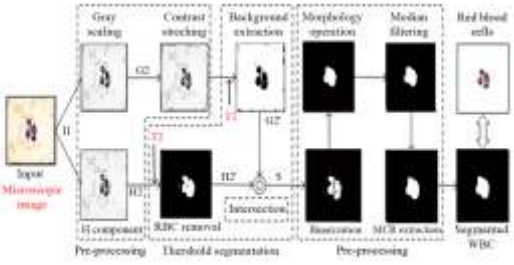


Fig.4 Block diagram of the enhanced dual-threshold segmentation.

The background separation, red blood cell extraction, and the finest threshold collection are the three key steps comprised by the threshold segmentation. The best threshold collection component uses the golden section search approach. Finally, in the post-processing stage, median filtering, and arithmetical morphology are utilised to remove noise and incomplete WBCs.

Image pre-processing

Two processed images are acquired during pre-processing for subsequent image segmentation processing. Figure 5b shows how the colour input image is converted to a grayscale image. Each member of the matrix[25] determines the intensity of each pixel. For convenience, most advanced digital files employ integers between 0 and 255, yielding 256 different grey levels. This number of grey levels is sufficient for working with medical images. The Image Contrast Stretching (ICS) is carried out by sliding a window over the image (known as the KERNEL) and altering the inner component using Eq. (1) below

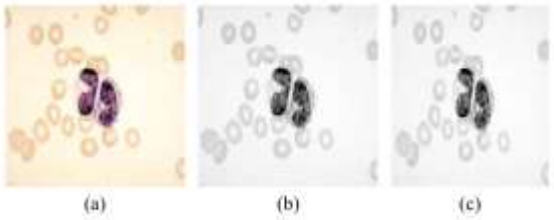


Fig. 5 (a) Original image, (b) grayscale image, and (c) image contrast stretching.

$$I_p(1+x) = \frac{255[I_o(x,y) - m_i]}{(m_a - m_i)} \qquad (1)$$

where p is the pixel organize of the picture; Ip is the differentiation-extending process's yield shading level for the pixel; The lowest and highest shading levels in the information picture are mi and ma, respectively. Io is the pixel's information shading level. Io(x, y) is the intensity of original image co-ordinates (x, y) in pixel

Threshold segmentation

The system's core consists of image thresholding applications for image segmentation. Thresholding, which is applied to a single picture, is the most basic method of segmenting an image. Thresholding[26] is a technique for creating binary pictures from a greyscale image. To isolate these modes from the background, set a T threshold that separates them. f (x, y) is the intensity or pixel value of the image at the point specified by the coordinates (x, y). Any image point (x, y) with f (x, y) > T is an object point; otherwise, the point is a background point. Equation (2) defines the threshold image g (x, y),

$$g(x,y) = \begin{cases} \text{A1, if } f(x,y) > T; \\ \text{B1, if } f(x,y) \leqslant T \end{cases} \qquad (2)$$

where pixel A1 denotes the items, whereas pixel B1 denotes the backdrop. Through conversion, A1 = 1 is assigned to the white color and B1 = 0 is assigned to the black color in the picture. The global threshold is regarded in the equation after the complete picture, T is considered an applicable constant. Variable thresholding refers to variations in T over the course of an image.

Dual thresholding

Two image characteristics are combined using dual thresholding. This technique divides the image based on histogram equalization [27]. G (x, y) provides a split

$$G(x,y) = \begin{cases} A, \text{ if } f(x,y) > T_2; \\ B, \text{ if } T_1 < f(x,y) \leqslant T_2; \\ C, \text{ if } f(x,y) \leqslant T_1 \end{cases} \qquad (3)$$

The split image (G) is formed by assigning different values (A, B, C) to pixels according to their intensity levels and the specified thresholds. To come up with an acceptable objective function, start with the Dice Similarity Coefficient (DSC), which is commonly employed to quantify segmentation impact. It is described as

$$\text{DSC}(C_1, D_1) = \frac{2(C_1 \cap D_1)}{(C_1 \cup D_1)} \qquad (4)$$

where C1 is the zone of the objective district of the aftereffect of a subsequently divided image, and D1 is the zone of the objective district of the ground truth image actuated by the physically portioned pictures. DSC varies by a factor between 0 and 1. According to this reality, the goal of work is determined by

$$DSC = f(\text{Threshold}_1, \text{Threshold}_2) \quad (5)$$

The issue of advancement is illustrated as follows: By selecting appropriate Threshold1 and Threshold2, the influence DSC will be as widespread as possible.

Post processing

White platelets can be divided after edge division. In the interim, binarization is used to transform the output image into a paired image, because it is still a grayscale image with some noise[28]. Then, morphological disintegration is utilised to fill tiny apertures, interface restricted holes, and expel small dabs, as well as the inadequate WBCs from the picture, in conjunction with middle separation and Maximum Connected Region (MCR) extraction procedures. The parallel image is next transformed into an RGB shaded image, but this step is optional.

Binarization

Binary images are frequently encountered in digital image processing tasks, often arising as masks or outcomes of various techniques like segmentation, thresholding, and dithering. Due to their straightforward nature, they find extensive use across different applications[29],

$$f(x,y) = \begin{cases} 1, \text{ if } f(x,y) > T; \\ 0, \text{ if } f(x,y) < T \end{cases} \quad (6)$$

Depending on the significance of the threshold T in the histogram, the image intensity may be divided intotwo distinct groups. Background pixels f (x, y) < T in the segmented binary picture have a value of zero, whereas object pixels f (x, y) > T have a value of one.

Morphological operation

Particularly in machine vision and autonomous object recognition, morphological processes are crucial to advanced digital image processing[29]. The Structuring Element (SE), controlled by a grid of 0 s and 1 s, determines the degree of thickening. The following Eq. (7) demonstrates how to describe dilation mathematically using set notation:

$$A \oplus A_s = \{z | (A'_s) z \cap A \neq \Phi\} \quad (7)$$

whereas A is the original image, As is the structuring element, represents the dilation of set A by scale factor s, and z is the resulting set and is an empty component. The action of dilation is commutative and well-known. By using an organizing component, Erosion contracts or decreases the objects in a double image. The numerical depiction of erosion is shown in the following:

$$A \oplus As = \{z | (A'_s) z \cap A_c \neq \Phi\} \quad (8)$$

command imerode is used to execute erosion in MATLAB (image name, SE). Erosion and dilation are often utilized in image processing and in different mixes. Morphological picture opening and closing are triggered by the collection of these two criteria. Morphological opening is represented as a disintegration activity followed by an expansion activity[26]. In Eqs. (9) and (10), the terms " X⊘Y " and "Y" stand for the morphological opening of the picture formed by X/Y, where the morphological opening is defined as the erosion of X by Y followed by dilatation of the resulting result,

$$X \oslash Y = (X \ominus Y) \oplus Y \quad (9)$$

$$X \bullet Y = (X \oplus Y) \oplus Y \quad (10)$$

where X Y X⊖Y represents the erosion of sets X and Y, represents the dilation of set X by set Y. denotes dilation and ⊖ denotes erosion[29]. Equation (11) demonstrates how an image f will first enlarge before eroding as a result of a structural component s,

$$f \oslash s = (f \ominus s) \oplus s \quad (11)$$

An opening is an idempotent job in which further openings with the same organizing component have no further influence on the picture after it has been opened,

$$(f \oslash s) \oslash s) = f \oslash s \quad (12)$$

In Eq. (13), the dilatation followed by erosion of an image f by a structuring element is represented,

$$f \cdot s = (f \oplus S_{\text{rot}}) \ominus S_{\text{rot}} \quad (13)$$

Feature extraction

The following feature extraction process uses the segmented information, as well as the spatial information of the segmented objects. The 2D-Haar wavelet transformation is used to extract features from the de-noised picture for decomposition, which extracts and maintains the low-level frequency components in the LL-sub band of the decomposed image[30].

Algorithm of Hybrid DWT for color features extraction

Figureing a colour feature is a group of bins that depict the distribution of colours in an image, with each bin corresponding to a colour in the quantized colour space[30]. In Eq. (14), a colour histogram for a particular image is represented as a vector

$$H = \{H[0], H[1], H[2], H[3], \ldots, H[I], \ldots, H[n]\} \quad (14)$$

The number of pixels in the image that contain colour I is represented by H [i], the number of bins in the colour histogram is represented by n, and I is the colour bin in the colour histogram which is the i-th element of pixel. Typically, a colour histogram bin is assigned to each pixel in an image[31]. The normalized colour histogram is shown in the following:

$$H' = \left\{H'[0], H'[1], H'[2], H'[3], \ldots, H'[i], \ldots, H'[n]\right\} \quad (15)$$

where , and p is the total number of pixels of an image.

Contrast

It is the measure of contrast between the intensity of a pixel and those of its neighbours throughout the whole ROI

$$\text{Contrast} \sum_i \sum_j (i-j)^2 C(i,j) \quad (16)$$

Where C (i, j) refers to the co-occurrence matrix, and the nested summations iterate over the indices i and j, i is the pixel's i-th element, and j is the pixel's j-th element.

Homogeneity

Homogeneity is defined as the difference between the distribution of elements in the Gray-Level Co occurrence Matrix (GLCM) and the GLCM of each ROI, with a value ranging from 0 to 1. It is referred to as

$$\text{Homogeneity} = \sum_i \sum_j \frac{C(i,j)}{1+|i-j|} \quad (17)$$

Mean

Mean is the arithmetic average of a set of values, and it is defined as

$$\text{Mean } (\mu) = \frac{\sum_i^n \sum_j^n C(i,j)}{M \times N'} \quad (18)$$

where μ is the mean. M is the number of rows, and N' is the number of columns in the array

Energy

The measure of the amount of pixel pair repeats is called energy (E). It assesses an image's consistency. The energy value is high when pixels are comparable,

$$\text{Energy } (E) = \sum_i \sum_j C(i,j)^2 \quad (19)$$

Area A(R) In Eq. (20), area is just the number of image pixels that make up the region R, N represents the value of area, which is equal to the number of elements in R,

$$A(R) = |R| = N \quad (20)$$

The Gaussian region equation for polygons, as illustrated in Eq. (21), may be used to calculate the area of a connected region (without holes)

$$A(R) \approx \frac{1}{2}\left|\sum_{i=0}^{M-1} (u_i \cdot v_{i+1} \bmod M - u_{i+1} \bmod M \cdot v_i)\right| \quad (21)$$

where M is the vertices of the polygon, ui and vi are co ordinates of the i-th vertex of the polygon.

Eccentricity

Eccentricity is a geometric property used in image analysis and classification to quantify the elongation or stretchiness of objects or regions within an image, which can be valuable in distinguishing between different classes or

categories of objects based on their shapes. It is expressed as

$$\mathrm{Ecc}(R) = \frac{a_1}{a_2} = \frac{\mu_{20} + \mu_{02} + \sqrt{(\mu_{20} - \mu_{02})^2 + 4\mu_{11}^2}}{\mu_{20} + \mu_{02} - \sqrt{(\mu_{20} - \mu_{02})^2 + 4\mu_{11}^2}} \quad (22)$$

respectively. μ20, μ02, μ11 are central moments. Feature extraction (GLCM) is a technique for suppressing the original image data set by measuring selected values or features that aid in classifying pictures. Color, form, and texture comprise the visual content of an image, but the semantic content is complicated and depends on the visual content[32]. 3.10 Classification The input space is divided into numerous local regions by fuzzy clustering. The computation complexity is reduced based on Euclidean distance, and the fuzzy rule number is determined by a validity function based on both the separation and the compactness among clusters. This improved adaptive neuro-fuzzy neural network[32] is used where all cell types from the microscopic blood cell dataset are examined. The dataset's microscopic blood images have a native resolution of 2592 pixel× 1944 pixel and are obtained with a Powershot G5 camera[33]. (1) Architecture To establish the architecture of an ANFIS, the first order Sugeno style Fuzzy Inference System (FIS) is initially introduced. The mapping from a given crisp input to a crisp output is controlled by fuzzy set theory in a first-order Sugeno style FIS model, as shown in the following:

$$x_1 \text{ is } A_1,\ x_2 \text{ is } A_2,\ \ldots,\ x_n \text{ is } A_n \quad (23)$$

$$y = k_0 + k_1 k_1 + k_2 k_2 + \cdots + k_n k_n \quad (24)$$

where x1, x2, ..., xn represent input signals, A1, A2, ..., An represent fuzzy sets, and y represents the output variable[31]. Find it in a fuzzy rule like this. The output variable[32] is a first-order polynomial input variable

Description of the method

An ANFIS is an ANN that is functionally equivalent to a first-order Sugeno style FIS. An ANFIS model consists of one input layer, four hidden layers, and one output layer, for a total of six levels. Signal forwarding is the responsibility of every layer. A similar ANFIS model is shown in Fig. 6. A network with two inputs, X and Y, and one output

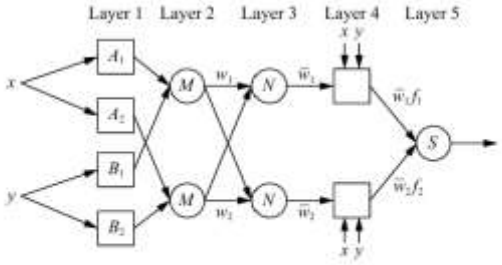


Fig. 6 Improved ANFIS architecture.

is assumed.

$$O_i^1 = \mu_{Ai}(x), \text{ for } i = 1, \text{ and } 2 \quad (26)$$

$$O_i^1 = \mu_{Bi}(x), \text{ for } i = 3, \text{ and } 4 \quad (27)$$

$$O_i^4 = \bar{w}_i f_i = \bar{w}_i\,(p_i x_1 + q_i x_2 + r_i x_3 + a_i x_4 + b_i x_5 + c_i x_6 + d_i x_7 + t_i) \quad (28)$$

IV EXPERIMENTAL RESULT

The study's findings are given and analysed in this chapter with regard to the study's goal, which is to examine the impact of employing visual representations of indications in microscopic blood cells[34−38]. The results and discussion related to the proposed work are also provided, including segmentation using enhances dual threshold, feature extraction using hybrid DWT classification, and I ANFIS. This study examines several classification algorithms, such as relevance vector machines, adaptive neuro-fuzzy inference systems, and k-nearest neighbors, for the categorization of microscopic blood cell data. Many computational analyses are carried out. The resulting prediction performances are comparable with those of already available methods. However, it is discovered that the suggested classification method, dubbed the I-ANFIS, performs significantly better than previous methods[39]

Performance measure

The suggested work's findings help in analysing the process' efficiency using microscopic blood

cell datasets. Performance measurement is the process of quantifying the efficiency and effectiveness of previous actions. To determine results, all performance measurement processes involve statistical modelling. A complete copy of an organization's performance can never be achieved since some parameters cannot be assessed directly and must be inferred by indirect observation, and a complete collection of records can never offer an evaluation without compression of crucial statistics. Enhanced Dual Threshold Segmentation (EDTS) is used for feature extraction to improve accuracy, precision, and recall. The results of comparing the F measure to dual threshold segmentation accuracy are listed in Table 1. Feature extraction aims to make models simpler and clearer, improves classification performance, and provides clean and intelligible data. A comparison of classification accuracy using various feature extraction algorithms is shown in Table 1. Table 2 shows the various segmentation and EDTS comparisons with Dual Threshold Segmentation (DTS) for all cell types, including band cells, metamyelocytes, myeloblasts, N. myelocytes, N. promyelocytes, and neutrophil cells. Figure 7 shows the EDTS comparison of segmentation accuracy performance for all cell types. Table 3 shows the comparison of the performance analysis of the proposed I-ANFIS. The performance analysis presented by I-ANFIS is compared to several classification approaches, ANFIS, KNN, and RVM, shown Fig. 8. The comparison of classification performance for various classification strategies is shown in Fig. 9. Table 4 compares the proposed I-ANFIS to ANFIS, KNN, and RVM in terms of performance

Discussion

The proposed algorithm for classifications is tested on the microscopic blood cell datasets. The experiments have been carried out to assess the following criteria: • To determine if the consistency measure and consistency factor are effective criteria for assessing the calibre of feature subsets produced. • To evaluate the accuracy, sensitivity, specificity, and classification performance analysis of classifiers with respect to the features obtained from the segmentation. • To evaluate the performance of the algorithm in terms of the classification accuracy needed to reach a good solution for leukemia detection

Table 1 Different segmentation and comparison of EDTS performance measure.

(%)

Cell type	DTS accuracy	EDTS accuracy	Precision	Recall	F-measure
Band cell	95.7264	96.3456	90.28	98.89	94.89
Metamyelocyte	88.0452	97.2896	88.55	98.45	98.00
Myeloblast	79.8480	89.5216	88.53	98.89	93.40
N. myelocyte	70.9344	92.5936	86.48	98.85	92.64
N. promyelocyte	70.0864	89.7856	87.68	98.96	93.37
Neutrophil cell	67.3392	94.8224	99.88	99.90	99.88

Table 2 Different segmentation and EDTS comparison for all cell types.

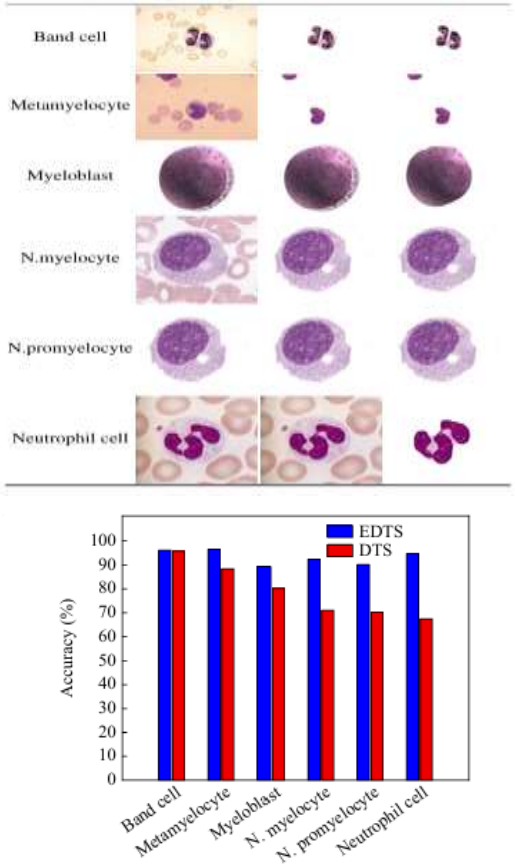


Fig. 7 Comparison of accuracy performance for EDTS.

Table 3 Comparison of performance analysis for the proposed I-ANFIS.

(%)

Algorithm	Accuracy	Sensitivity	Specificity
I-ANFIS	97.1429	0.9600	0.9000
ANFIS	94.2857	0.9200	0.9000
KNN	91.4286	0.8800	0.9000
RVM	82.8571	0.8000	0.8000

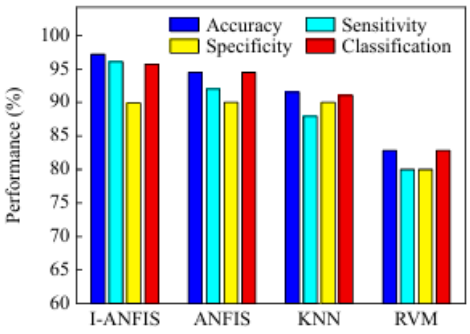


Fig. 8 Comparison of performance analysis for the proposed technique.

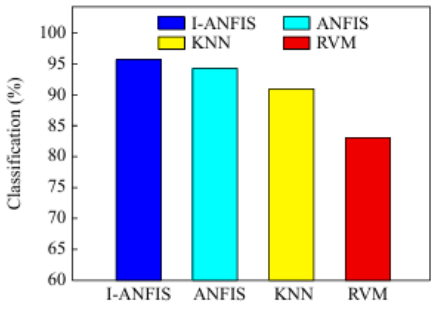


Fig. 9 Comparison of classification performance for the proposed technique.

Table 4 Comparison of classification performance for the proposed I-ANFIS

(%)

Algorithm	Accuracy
I-ANFIS	95.67
ANFIS	94.29
KNN	91.05
RVM	82.86

technique can provide the maximum accuracy for all cell types and microscopic datasets of the same domain, the best feature extraction strategy for a given dataset depends on the quantity, type, and occurrences of attributes. I-ANFIS can be used to increase the proposed classifier's accuracy once the best feature extraction method for a specific dataset has been identified. In the world of medical diagnostics, accuracy is crucial for diagnosing leukemia. Experiments demonstrate that using feature extraction as a pre processing strategy improves classification accuracy significantly. It also concludes that using EDTS feature extraction improves the classifier's accuracy, sensitivity, specificity, and classification. This comparative analysis chapter discusses and displays the performance measure and performance bar. Different classification algorithms are compared to the proposed I-ANFIS classification using microscopic blood cell datasets. The suggested classification approach, I-ANFIS, outperforms the competition in terms of accuracy, sensitivity, specificity, and classification metrics. This work aids in the diagnosis of leukemia by physicians and healthcare professionals

V CONCLUSION

In conclusion, this research presents a novel approach for discriminating between normal and acute lymphoblastic leukaemia in bone marrow samples. The proposed method incorporates an enhanced dual threshold segmentation technique, accurate nucleus and cytoplasm segmentation, feature extraction using hybrid discrete wavelet transform, and classification utilizing the I-ANFIS. By utilizing microscopic images of blood cells obtained from the ALL-IDB2 databases, the I-ANFIS machine learning system effectively classifies normal and leukemic blood cells based on the extracted characteristics. The proposed approach addresses the issue of class imbalance and demonstrates its efficacy through evaluation metrics such as accuracy, sensitivity, specificity, and classification performance comparison with existing methods. Looking ahead, future research can explore additional avenues and research directions within the scope of this I-ANFIS classification investigation. Specifically, adapting the proposed strategy to other machine learning approaches with additional adjustable parameters holds potential for further improvement and

exploration. In summary, this research presents a comprehensive method for automatic segmentation, feature extraction, and classification of bone marrow samples to differentiate between normal and acute lymphoblastic leukaemia. The proposed approach offers enhanced classification performance, as well as improved speed and accuracy, compared to alternative methods, making it a promising tool for medical diagnosis in this domain

REFERENCES

[1] S. Bandini, L. Vanneschi, A. Wuensche, and A. B. Shehata, "Cellular automata pattern recognition and rule evolution through a neuro-genetic approach," *J. Cellular Automata*, vol. 4, no. 3, pp. 171–181, 2009.

[2] D. G. Aguilera and J. G. Lahoz, "Learning from educational software in 3D cartography," *British Journal of Educational Technology*, vol. 39, no. 4, pp. 726–731, 2008.

[3] F. Golchin and K. K. Paliwal, "Quadtree-based classification in subband image coding," *Digital Signal Processing*, vol. 13, no. 4, pp. 656–668, 2003.

[4] F. Qadir, M. A. Peer, and K. A. Khan, "An effective image noise filtering algorithm using cellular automata," in *Proc. Int. Conf. Computer Communication and Informatics*, Coimbatore, India, 2012, pp. 1–5.

[5] H. T. Madhloom et al., "An automated white blood cell nucleus localization and segmentation using image arithmetic and automatic threshold," *Journal of Applied Sciences*, vol. 10, no. 11, pp. 959–966, 2010.

[6] V. A. Kovalev, A. Y. Grigoriev, and H. S. Ahn, "Robust recognition of white blood cell images," in *Proc. 13th Int. Conf. Pattern Recognition*, Vienna, Austria, 1996, pp. 371–375.

[7] F. Scotti, "Robust segmentation and measurement techniques of white cells in blood microscope images," in *Proc. IEEE Instrumentation and Measurement Technology Conf.*, Sorrento, Italy, 2006, pp. 43–48.

[8] V. Piuri and F. Scotti, "Morphological classification of blood leucocytes by microscope images," in *Proc. IEEE Int. Conf. Computational Intelligence for Measurement Systems and Applications*, Boston, MA, USA, 2004, pp. 103–108.

[9] N. H. A. Halim, M. Y. Mashor, and R. Hassan, "Automatic blasts counting for acute leukemia based on blood samples," *International Journal of Research and Reviews in Computer Science*, vol. 2, no. 4, pp. 971–976, 2011.

[10] S. Mohapatra, D. Patra, and S. Satpathy, "An ensemble classifier system for early diagnosis of acute lymphoblastic leukemia in blood microscopic images," *Neural Computing and Applications*, vol. 24, nos. 7–8, pp. 1887–1904, 2014.

[11] R. D. Labati, V. Piuri, and F. Scotti, "All-IDB: The acute lymphoblastic leukemia image database for image processing," in *Proc. IEEE Int. Conf. Image Processing*, Brussels, Belgium, 2011, pp. 2045–2048.

[12] Vikram, S. (2023). Enhancing Credential Security in Distributed Manufacturing: Machine Learning for Monitoring and Preventing Unauthorized Client Certificate Sharing. JOURNAL OF ADVANCE AND FUTURE RESEARCH, 1(7). https://doi.org/10.56975/jaafr.v1i7.501709.

[13] J. Angulo and G. Flandrin, "Microscopic image analysis using mathematical morphology: Application to haematological cytology," in *Science, Technology and Education of Microscopy: An Overview*, A. Méndez-Vilas, Ed. Badajoz, Spain: Formatex, 2003, pp. 304–312.

[14] N. Sinha and A. G. Ramakrishnan, "Blood cell segmentation using EM algorithm," in *Proc. Indian Conf. Computer Vision, Graphics & Image Processing*, Ahmadabad, India, 2002.

[15] N. Theera-Umpon, "Patch-based white blood cell nucleus segmentation using fuzzy clustering," *ECTI Transactions on Electrical Engineering, Electronics, and Communications*, vol. 3, no. 1, pp. 15–19, 2005.

[16] Mahesh Ganji. (2025). Enhancing Oracle Cloud HR Reporting Through AI-Driven Automation. Journal of Science & Technology, 10(6), 28–36. https://doi.org/10.46243/jst.2025.v10.i06.pp28-36.

[17] D. Comaniciu and P. Meer, "Cell image segmentation for diagnostic pathology," in *Advanced Algorithmic Approaches to Medical Image Segmentation*, London, UK: Springer, 2002, pp. 541–558.

[18] L. Yang, P. Meer, and D. J. Foran, "Unsupervised segmentation based on robust estimation and color active contour models," *IEEE Transactions on Information Technology in Biomedicine*, vol. 9, no. 3, pp. 475–486, 2005.

[19] Mallick, P. (2025). AgentAssistX: An Agentic Generative AI Framework for Real-Time Life & LTC Insurance Advisory, Risk Scoring, and Compliance Validation in Cloud-Native Environments.

[20] Todupunuri, A. (2025). Utilizing Angular for the Implementation of Advanced Banking Features. SSRN Electronic Journal. https://doi.org/10.2139/ssrn.5283395.

[21] S. Wang and M. Wang, "A new detection algorithm based on fuzzy cellular neural networks for white blood cell detection," *IEEE Transactions on Information Technology in Biomedicine*, vol. 10, no. 1, pp. 5–10, 2006.

[22] S. Chinwaraphat et al., "A modified fuzzy clustering for white blood cell segmentation," in *Proc. Int. Symp. Biomedical Engineering*, Changsha, China, 2008, pp. 356–359.

[23] C. Meurie et al., "Combination of multiple pixel classifiers for microscopic image segmentation," *International Journal of Robotics and Automation*, vol. 20, no. 2, pp. 63–69, 2005.

[24] M. Ghosh et al., "Statistical pattern analysis of white blood cell nuclei morphometry," in *Proc. IEEE Students Technology Symp.*, Kharagpur, India, 2010, pp. 59–66.

[25] B. C. Ko, J. W. Gim, and J. Y. Nam, "Automatic white blood cell segmentation using stepwise merging rules and gradient vector flow snake," *Micron*, vol. 42, no. 7, pp. 695–705, 2011.

[26] Todupunuri, A. (2025). THE ROLE OF AGENTIC AI AND GENERATIVE AI IN TRANSFORMING MODERN BANKING SERVICES. American Journal of AI Cyber Computing Management, 5(3), 85–93. https://doi.org/10.64751/ajaccm.2025.v5.n3.pp85-93.

[27] Rongali, L. P. (2025). Performance Overhead and Optimization Strategies in Opentelemetry. https://doi.org/10.36227/techrxiv.175790708.84315250/v1.

[28] Gaddam, S. (2025). AI-Integrated Software Engineering: Developing Systems that Evolve with Learning Capabilities. Journal of Information Systems Engineering and Management, 10(63s)..

[29] R. Seshadri et al., "A morphometric classification of acute lymphoblastic leukemia in children," *Medical and Pediatric Oncology*, vol. 13, no. 4, pp. 214–220, 1985.

[30] J. Angulo, J. Serra, and G. Flandrin, "Quantitative descriptors of the lymphocytes," *Analytical Cellular Pathology*, vol. 22, nos. 1–2, pp. 69–70, 2001.

[31] J. Angulo, J. Klossa, and G. Flandrin, "Ontology-based lymphocyte population description using mathematical morphology on colour blood images," *Cellular and Molecular Biology*, vol. 52, no. 6, pp. 2–15, 2006.

[32] L. Gupta et al., "Identification of different types of lymphoblasts in acute lymphoblastic leukemia using relevance vector machines," in *Proc. IEEE Engineering in Medicine and Biology Society*, 2009.

[33] H. J. Escalante et al., "Acute leukemia classification by ensemble particle swarm model selection," *Artificial Intelligence in Medicine*, vol. 55, no. 3, pp. 163–175, 2012.

[34] B. Swolin et al., "Differential counting of blood leukocytes using automated microscopy and ANN-based decision support," *Clinical and Laboratory Haematology*, vol. 25, no. 3, pp. 139–147, 2003.